Branching Ratio between Proton Transfer and Electron Transfer Channels of a Bidirectional Proton−Coupled Electron Transfer

ARTICLE *in* JOURNAL OF PHYSICAL CHEMISTRY LETTERS · MARCH 2014

Impact Factor: 7.46 · DOI: 10.1021/jz500396r

2 AUTHORS, INCLUDING:

Kyoung Koo Baeck
Gangneung-Wonju National University
44 PUBLICATIONS **425** CITATIONS

THE JOURNAL OF PHYSICAL CHEMISTRY Letters

Letter

pubs.acs.org/JPCL

Branching Ratio between Proton Transfer and Electron Transfer Channels of a Bidirectional Proton-Coupled Electron Transfer

Heesun An and Kyoung Koo Baeck*

Department of Chemistry, Gangneung-Wonju National University, Gangneung, Gangwondo, 210-702, Korea

Supporting Information

ABSTRACT: Rigorous quantum dynamical study of concerted proton-coupled electron transfer (PCET) on the time scale of a few femtoseconds (fs) has been rarely reported. Herein, a time-dependent quantum wavepacket propagation method was applied to the dynamics of the charge-transfer excited electronic state of FHCl corresponding to F^+HCl^-. The dynamics corresponds to a bidirectional PCET with two dissociation channels: the electron transfer (ET, generating FH+Cl) and proton transfer (PT, generating F+HCl) paths. The calculated branching ratio (Cl/F), 0.78, implies a surprising fact: PT prevails over ET. A detailed analysis of the proton movement and electron readjustment suggests that the proton movement starts ∼3 fs earlier than the electron movement, and the electron readjustment is triggered by the initial movement of the proton. The branching ratio drastically inverts to 1.24 because of a reduced nonadiabatic effect in the isotope-substituted system, FDCl.

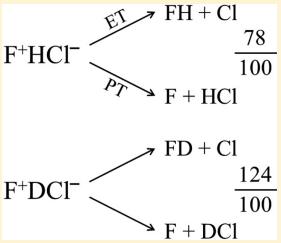

SECTION: Kinetics and Dynamics

Recently, proton-coupled electron transfer (PCET) has attracted special interest because it is one of the most essential ingredients in studying diverse physical, chemical, and biological processes. Despite numerous recent theoretical and experimental studies on PCET,[1−4] most of them were studied from a kinetics perspective. The rigorous quantum dynamical study of the detailed movement of proton and the concomitant redistribution of electron on the time scale of a few femtoseconds (fs) has been rarely reported. Actual overall PCET processes comprise a few elementary steps: a stepwise sequence of electron transfer (ET) followed by proton transfer (PT); a similar sequence, but in the reverse order; a concerted PCET; and H-atom transfer (HAT).[1−4] Moreover, ET/PT can be either unidirectional or bidirectional.[2,4] However, the classification is mainly based on kinetics that are manageable by current experimental techniques, i.e., in the range of at least ∼100 fs. Independent theoretical and experimental studies of such elementary steps in the shorter time scale can provide augmenting insights to the kinetic theory of PCET under active study nowadays.[1−4] Among the elementary steps, the concerted PCET step is particularly important and cumbersome because this step plays the key role in excited-state PCET processes,[1−5] and a simple combination of individual theories of ET and PT is not sufficient.

In this work, the dynamics of the charge-transfer (CT) state of FHCl, corresponding to a bidirectional concerted PCET, was studied by a rigorous quantum mechanical method with special emphasis on the PT and ET on the time scale of a few fs. The precursor, $FHCl^-$ (S_0), is a weakly bound system between FH and Cl^-, and the electron photodetachment from the Cl^- part produces the ground electronic state, D_0, of the neutral FHCl, which undergoes simple dissociation to the neutral FH and Cl fragments (Figure 1). However, the photodetachment of an electron from the F part produces the first excited electronic state, D_1, of the neutral FHCl corresponding to the CT state with F^+H-Cl^- characteristic. Two reaction channels are now opened because of the nonadiabatic coupling between D_1 and D_0. The neutral F and HCl fragments (r.h.s. of Figure 1) resulted from the PT from the F^+H moiety to Cl^- followed by the dissociation of the F−HCl bond. In contrast, the neutral FH and Cl fragments (l.h.s. of Figure 1) resulted from the ET from Cl^- to F^+H followed by the FH−Cl bond dissociation.

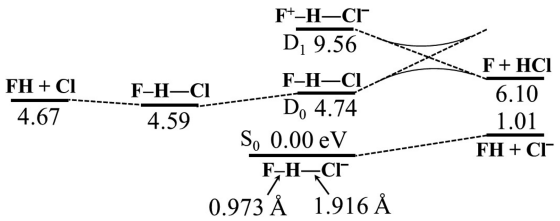

Figure 1. The relative energies (in eV), without ZPE correction, of the dissociation limits (FH + Cl, F + HCl, and FH + Cl^-), stationary structures, and vertical energies of D_0 (4.74) and D_1 (9.56) with respect to the S_0 state of $FHCl^-$ are obtained by using the ωB97XD, the MRCISD+Q, and the IP-EOMCC methods.

The time-dependent quantum wavepacket propagation method within a properly chosen dimensional space is one of the most rigorous methods that include both the tunneling effect of proton and the nonadiabatic effect between electronic states.[6] According to our preliminary studies, the adiabatic potential energy surfaces (PESs) of all the three electronic states (S_0, D_0, and D_1) have a linear molecular configuration as the stationary structure. The coincidence of the linearity is the

Received: February 23, 2014
Accepted: March 24, 2014
Published: March 24, 2014

   dx.doi.org/10.1021/jz500396r | J. Phys. Chem. Lett. 2014, 5, 1307−1311

pertinent feature that uses the reduced two-dimensional (2D) space defined by the two bond lengths, R_{FH} and R_{HCl}.

The adiabatic 2D PES of $FHCl^-$ was constructed by using the ωB97XD/aug-cc-pVTZ method[7] implemented in the Gaussian 09 program[8] (Supporting Information, Part-1 for ab initio computations). Then, the time-dependent Schrodinger equation was solved by using the kinetic operator for colinear three-atomic systems.[6] The wavepackets of the lowest vibration level was obtained by applying Chebysev's imaginary time propagator method[9] implemented in the WavePacket program.[10] The first panel of Figure 3 shows the wavepacket of $FHCl^-$ drawn on the top of the contour representation of the diabatic V_{22} state (*vide infra*) to emphasize the situation immediately after the photodetachment of the precursor anion up to the CT state, D_1 (V_{22}). On the other hand, the adiabatic energies of the D_0 and D_1 states of the neutral FHCl were calculated by using the MRCISD+Q method implemented in the MOLPRO program[11] with the aug-cc-pVTZ basis sets. Note that the ωB97XD-DFT was used for the anionic state (S_0), whereas the MRCISD+Q was used for the neutral states (D_0 and D_1). Details of the MRCISD+Q calculations are almost the same as those described in the ref 12 The vertical energy differences among the S_0, D_0, and D_1 states at the equilibrium geometry of the S_0 state were also calculated and confirmed by using the IP-EOMCC method[13] implemented in the ACES-II program[14] (Supporting Information, Part-2 for adiabatic PESs).

The nonadiabatic effect between the D_0 and D_1 states was treated by constructing the diabatic electronic states and the coupling term between them,[15] because the inclusion of the first-order nonadiabatic coupling term with adiabatic electronic state was not sufficient; it was shown that the second-order nonadiabatic term contributed ~30% of the total nonadiabatic effect in the dynamics of the CT state of NH_3Cl system.[16] The semidiabatization of our study[17] successfully reproduced the previous result[16] obtained with the first-order and second-order nonadiabatic coupling terms. Therefore, the diabatic 2D PESs and the coupling term of FHCl system were constructed from the adiabatic PESs of the MRCISD+Q calculations by applying the same procedure used in our previous study on the NH_3Cl system.[17] (Supporting Information, Part-3 for details of diabatic 2D PESs (V_{11}, V_{22}) and the coupling term V_{12}.)

To study the dynamics, the wavepacket of the precursor anion was vertically excited to the CT state, D_1 (V_{22}), of the neutral FHCl, and its time propagation was obtained by solving the time-dependent Schrodinger equation using the split-operator method[18] implemented in the Wavepacket program.[10] A damping function was placed at R_{FH} = 5.8 Å and R_{HCl} = 6.0 Å to absorb the dissociating wavepackets; other details are the same as those in our previous study.[19] The change in the populations of the two diabatic states up to 400 fs are shown in Figure 2 for FHCl and FDCl, with the insets showing more details during the earlier time of up to 50 fs.

The branching ratio (Cl/F) between the two dissociation channels was calculated after the propagation up to 400 fs, because the ratio was almost constant after 200 fs (Supporting Information, Part-4). The calculated ratio of FHCl, 0.72, is very interesting and surprising because the ratio, <1, implies that the PT channel (generating F atom and HCl) prevails over the ET path (generating FH and Cl atom). Because the process described here is an elementary step in terms of kinetics, the ET path is expected to be favored over the PT path. The relative energies of the two dissociation limits, as shown in Figure 1, also expect that the ET path is thermodynamically more favored over the other. However, our result contradicts both the expectations.

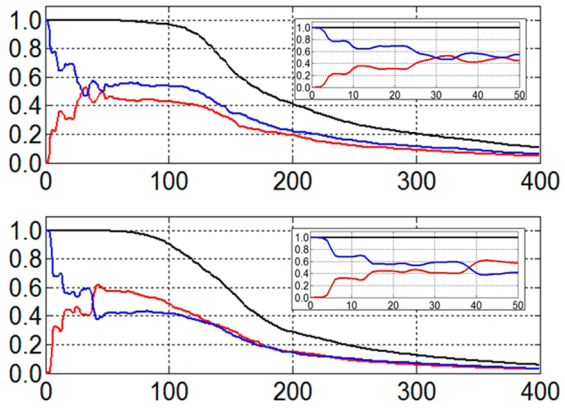

Figure 2. Change in the populations on V_{11} (red) and V_{22} (blue) after the vertical excitation of the vibration wavepacket of the anion precursor up to the CT state (D_1) of the neutral (a) FHCl (upper) and (b) FDCl (lower). The black line shows the decrease in the total population due to the dissociations. Details up to 50 fs are shown in the insets.

To understand the reason behind this finding, we investigated the PCET process in the range of the shorter time scale. Several snapshots of the time-propagating wavepackets on two diabatic PESs up to 30 fs are shown in Figure 3. Because the center of the propagating wavepacket moves along the line shown by the left-slanted dots, the one-dimensional (1D) cut of the 2D PESs along the dotted line is also drawn below the corresponding pair of contour maps. Notably, the dotted line moves slightly toward the upper right direction as the propagating time continues, because the distance between F and Cl nuclei increases gradually.

The snapshots in Figure 3 show an initial back-and-forth movement of the proton. The period of this first movement, ~12 fs, reflects the curvature of the V_{22} PES along the dotted line at the lowest energy point. Because of the gradual increase in the distance between the F and Cl nuclei during the first back-and-forth movement, the period of the subsequent cycles increased slightly. The regularity of the cycle was also diminished noticeably by the spreading of the wavepacket over a wide range of space, as can be estimated from the snapshots from 12 to 24 fs shown in Figure 3 and the change in the populations shown by the inset in Figure 2a. The roles and effects of the first movement of proton (and the concomitant change in the electron distribution) in the shorter time scale should be analyzed and emphasized more from Figure 4.

Immediately after the vertical excitation to the CT state at 0 fs, region **I** in Figure 4, the system corresponds to F^+H-Cl^-. The propagating wavepacket arrives at the nonadiabatic region, **II**, after 3 fs and makes the first bifurcation. The populations at 5−6 fs, shown in the inset of Figure 2a, indicate that ~80% population propagates along the V_{22} diabatic PES (the blue line in Figure 4), whereas ~20% population propagates along the V_{11} PES (the red line). The two bifurcated wavepackets arrive at regions **IV** and **V**, respectively, at 6 fs. The nuclear configurations now correspond to F—H−Cl because the FH distance increases with decreasing HCl distance.

Because the propagation along the V_{22} diabatic PES corresponds to a diabatic PT, the electronic nature of the wavepacket at region **III** corresponds to $F—{}^+H-Cl^-$, indicating that only the proton is transferred from the F^+H moiety to the

dx.doi.org/10.1021/jz500396r | J. Phys. Chem. Lett. 2014, 5, 1307−1311

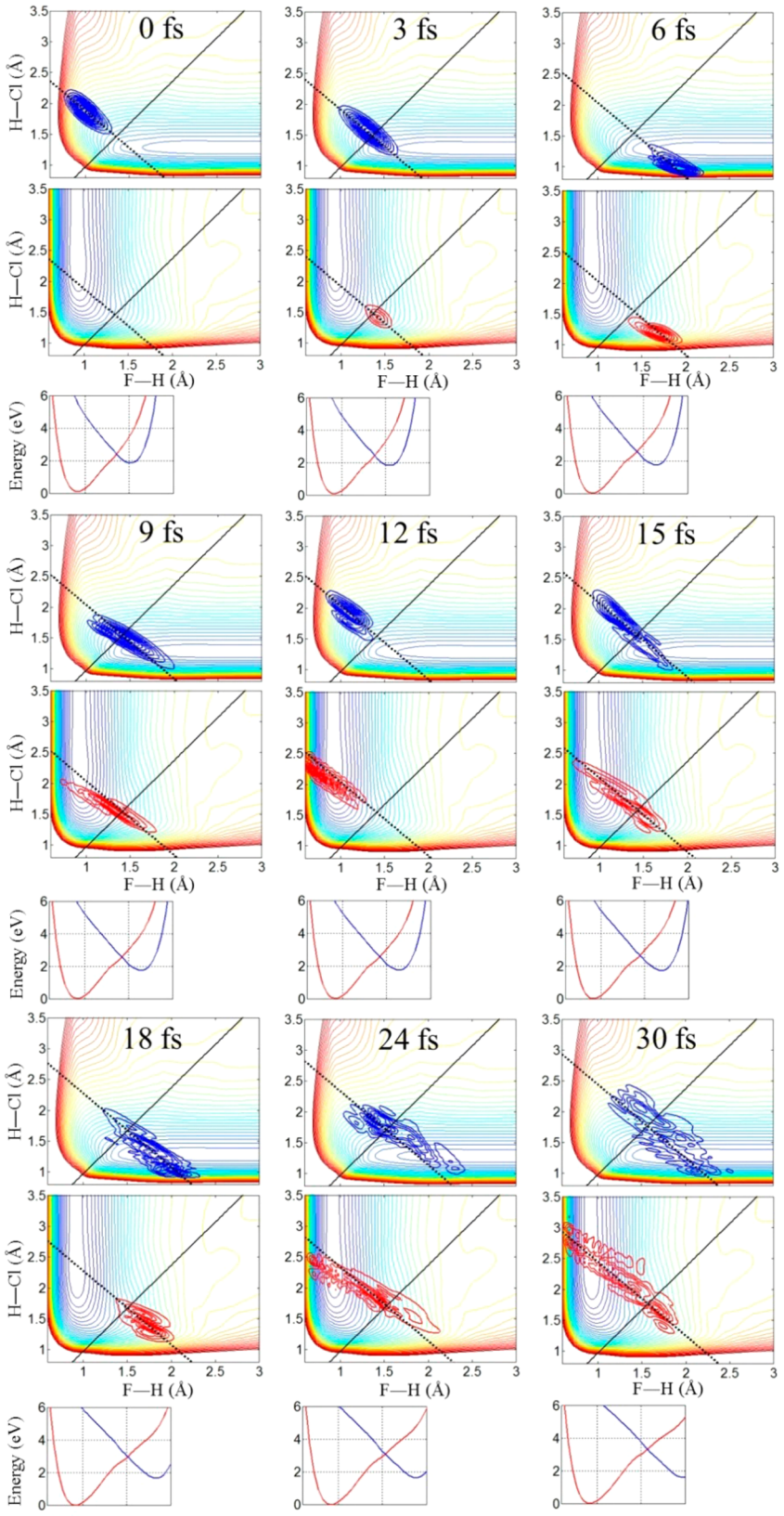

Figure 3. Snapshots of the propagating wavepackets. The upper (in blue) and lower (in red) contours of each pair represent the wavepackets on V_{22} (the CT state) and V_{11} diabatic PESs, respectively. The crossing points between the two diabatic PESs are shown by the right-slanted diagonal solid line, while the main path of the propagating wavepackets is shown by the left-slanted dotted line. The 1D cut along the dotted line, shown below each pair of contours, shows the changes in V_{22} (blue) and V_{11} (red) PESs.

Cl^- part, leaving its electron behind on the F nucleus. The subsequent rearrangement of the electron from the Cl^- part to the incoming proton during the change from **III** to **IV** affords the neutral HCl moiety, and its departure from the F would

dx.doi.org/10.1021/jz500396r | *J. Phys. Chem. Lett.* 2014, 5, 1307−1311

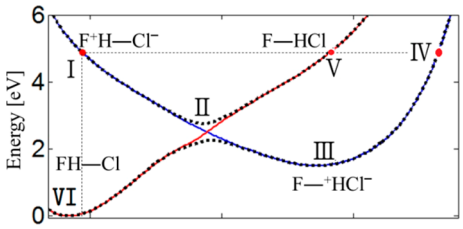

Figure 4. Changes in the characteristics of the electronic states during the early time dynamics. The dots (black) represent the adiabatic PESs by the MRCISD+Q/aug-cc-pVTZ method, whereas the solid curves (V_{11} and V_{22} by red and blue, respectively) represent the diabatic PESs. Herein, the horizontal coordinate corresponds to the left-slanted dotted line of the first panel of Figure 3. The bond lengths are R_{FH} = 0.973 Å and R_{HCl} = 1.916 Å at **I**, R_{FH} = 1.439 Å and R_{HCl} = 1.582 Å at **II**, R_{FH} = 2.338 Å and R_{HCl} = 0.940 Å at **IV**, and R_{FH} = 1.920 Å and R_{HCl} = 1.239 Å at **V**.

generate the F and HCl fragments. However, the separation does not occur immediately, as discussed below. On the other hand, the diabatic V_{11} PES corresponds to the FHCl electronic nature, and the electronic feature of the wavepacket in region **V** is F—H−Cl, indicating that the proton of the F^+H moiety moves toward the Cl^- part with simultaneous movement of the excess electron of the Cl^- part toward the incoming proton: the genuine concerted bidirectional PT/ET.

The direction of the propagation is inverted at 6 fs on both the diabatic PESs, and the reflected wavepackets propagate on V_{11} and V_{22} PESs. They make the second bifurcation again at 9 fs (region **II**), and reach near the initial position (**I** and **VI**) at 12 fs. The changes in the populations from 9 to 10 fs show the second stepwise change because of the second bifurcation: the increase in the population on V_{11} PES and the decrease on V_{22} PES, as shown by the red and blue lines, respectively, in the insets of Figure 2a. The change from region **V** (F—H−Cl) to region **VI** (F−H—Cl) along V_{11} PES corresponds to the HAT, whereas the transfer from region **IV** to region **VI** can be attributed to the tunneling of H atom from V_{22} PES to V_{11} PES. The transfer of populations from region **IV** to region **VI** by the tunneling is the main source for the increase in the population on V_{11} PES and the corresponding decrease on V_{22} PES—the increase in the population of V_{11} PES from ∼20% at 6 fs to ∼40% at 12 fs. The overall change from region **I** ($F-{}^+H—Cl^-$) to region **VI** (F−H—Cl) via not only **III** (**IV**) but also **V** can be regarded as resulting from the electron movement by the involvement of the proton movement. In other words, *the electron's adjustment is triggered by the initial movement of the proton*. The wavepacket, returned to region **I**, is reflected again there, and starts the subsequent second cycle. The amplitude of the proton movement during the period, 0.81−1.17 Å, is much larger than the amplitude of the usual vibrations and deserves to be studied in future experimental studies.

The population changes in the FDCl case, as shown in Figure 2b, indicate very similar patterns with three main differences from those of FHCl. The first is the increase in the period of the first cycle from 12 fs (FHCl) to 17 fs (FDCl). The second is the decrease in the portion of the diabatic PT from region **I** to region **III** from 80% (FHCl) to 70% (FDCl). The third is the inversion of the branching ratio (Cl/F) from 0.72 (FHCl) to 1.24 (FDCl). The inversion is so significant that it can be easily detected in the future experiments. The effective speed of the wavepacket propagation slows because of the increased reduced mass μ of FDCl, and the reduced speed accounts for the decreased nonadiabatic effect and the inverted branching ratio.

One of the most important findings of this study is the branching ratio, which indicates that the proton moves first and is followed by the electron's movement or adjustment even though the time gap is just ∼3 fs, the elapsed time of the first movement of wavepacket from region **I** to **II** in Figure 4. Moreover, the ET from the Cl^- part to the F^+H moiety may be triggered by the initial movement of the proton. This finding may seem contradictory to the common sense that the movement of electrons is faster than that of the proton. However, this finding simply indicates that *the PT starts earlier than ET in this bidirectional PCET process*. Because the first stage at 0 fs corresponds to $F^+H—Cl^-$, the positive charge at the *F* nucleus may affect the nearby proton earlier than the electrons near the Cl nucleus. In addition to the large nonadiabatic effect at region **II** shown in Figure 4, this earlier start of the PT affords a final branching ratio of 0.78, corresponding to the dominance of the PT over the ET. Although the time gap, between the start of the PT and that of ET, is very short to be easily confirmed by the usual experimental techniques, the recent advent of the attosecond science may be able to solve this.[20,21]

According to semiclassical treatments, the effective time scale for proton tunneling may be shorter than the effective time scale for the electronic transition in some PCET reactions.[22] However, the relevance of these relative time scales to the present work is unclear and needs to be examined further with another recent theoretical method[23] as well as recent experimental techniques.[20,21,24]

The extension of this study to full three-dimensional (3D) space can make a slight change in the quantitative aspects; however, the qualitative aspects may not change because the FHCl system corresponds to a heavy−light−heavy system, and its excited-state dynamics is initiated by the movement of not the heavy but the light particle. The momentum transferred to the F or Cl part by the initial movement of the proton is not sufficient to produce any significant effect on the bending movement within several tens of femtoseconds. It is noteworthy that all the larger PCET systems also correspond to the heavy−light−heavy system, and the masses of their heavy parts are even much higher than those of the F and Cl of the FHCl system. Therefore, the initial back-and-forth staggering movement of the proton may become more prominent with several more oscillations in the actual PCET cases.

The generality of our new finding in other PCET processes is an open question, and further rigorous quantum mechanical studies in the range of shorter time scale should be conducted for different cases. Our theoretical discussion about the time gap between the initial proton movement and the following electron adjustment is tentative and needs further theoretical and experimental studies.

■ ASSOCIATED CONTENT

Supporting Information

Part-1 for details of ab initio computations, Part-2 for adiabatic PESs, Part-3 for diabatic PESs and the coupling term between the diabatic PESs, and Part-4 for the change in the dissociation probabilities. This information is available free of charge via the Internet at http://pubs.acs.org/.

AUTHOR INFORMATION

Corresponding Author

*E-mail: baeck@gwnu.ac.kr.

Notes

The authors declare no competing financial interest.

ACKNOWLEDGMENTS

This study was supported by the grant (2013-022328) of the National Research Foundation of Korea, and by the Research Institute of Natural Science of Gangneung-Wonju National University. The computation time of this study was supported by the Supercomputing Center of Korea Institute of Science and Technology Information (KISTI) with supercomputing resources including technical support.

REFERENCES

(1) Cukier, R. I.; Nocera, D. G. Proton-Coupled Electron Transfer. *Annu. Rev. Phys. Chem.* **1998**, *49*, 337−367.

(2) Huynh, M. H. V.; Meyer, T. J. Proton-Coupled Electron Transfer. *Chem. Rev.* **2007**, *107*, 5004−5064.

(3) Hammes-Schiffer, S.; Stuchebrukhov, A. A. Theory of Coupled Electron and Proton Transfer Reactions. *Chem. Rev.* **2010**, *110*, 6939−6960.

(4) Hammes-Schiffer, S. Proton-Coupled Electron Transfer: Classification Scheme and Guide to Theoretical Methods. *Energy Environ. Sci.* **2012**, *5*, 7696−7703.

(5) Demchenko, A. P.; Tang, K.; Chou, P. Excite-State Proton Coupled Charge Transfer Modulated by Molecular Structure and Media Polarization. *Chem. Soc. Rev.* **2013**, *42*, 1379−1408.

(6) Tannor, D. J. *Introduction to Quantum Mechanics: A Time-Dependent Perspective*; University Science Books: Sausalito, CA, 2007.

(7) Chai, J. −D.; Head-Gordon, M. Long-Range Corrected Hybrid Density Functionals with Damped Atom−Atom Dispersion Corrections. *Phys. Chem. Chem. Phys.* **2008**, *10*, 6615−6620.

(8) Frisch, M. J.; Trucks, G. W.; Schlegel, H. B.; Scuseria, G. E.; Robb, M. A.; Cheeseman, J. R.; Scalmani, G.; Barone, V.; Mennucci, B.; Petersson, G. A.; et al., *Gaussian 09*, revision A.1; Gaussian, Inc.: Wallingford, CT, 2009.

(9) Kosloff, R.; Tal-Ezer, H. A Direct Relaxation Method for Calculating Eigenfunctions and Eigenvalues of the Schrödinger Equation on a Grid. *Chem. Phys. Lett.* **1986**, *127*, 223−230.

(10) Schmidt, B.; Lorenz, U. *WavePacket 4.7*: A program package for quantum-mechanical wavepacket propagation and time-dependent spectroscopy, available via http://wavepacket.sourceforge.net.

(11) Werner, H. −J.; Knowles, P. J.; Knizia G.; Manby, F. R.; Schütz, M.; Celani, P.; Korona, T.; Lindh, R.; Mitrushenkov, A.; Rauhut, G.; et al., *MOLPRO*, version 2012.1. A package of ab initio programs; see http://www.molpro.net.

(12) Deskevich, M. P.; Hayes, M. Y.; Takahashi, K.; Skodje, R. T.; Nesbitt, D. J. Multireference Configuration Interaction Calculations for the $F(^2P)+HCl\rightarrow HF+Cl(^2P)$ Reaction: A Correlation Scaled Ground State ($1^2A'$) Potential Energy Surface. *J. Chem. Phys.* **2006**, *124*, 224303−12.

(13) Nooijen, M.; Snijders, J. G. Second Order Many-Body Perturbation Approximations to the Coupled Cluster Green's Function. *J. Chem. Phys.* **1995**, *102*, 1681−1688.

(14) Stanton, J. F.; Gauss, J.; Perera, S. A.; Watts, J. D.; Yau, A. D.; Nooijen, M.; Oliphant, N.; Szalay, P. G.; Lauderdale, W. J.; Gwaltney, S. R.; et al., *ACES-II*: A Program Product of Quantum Theory Project, Release 2.5.0; University of Florida: Gainesville, FL, 2006.

(15) Baer, M. *Beyond Born-Oppenheimer: Electronic Nonadiabatic Coupling Terms and Conical Intersections*; Wiley-Interscience, Hoboken, NJ, 2006.

(16) Ronen, S.; Nachtigallova, D.; Schmidt, B.; Jungwirth, P. Nonadiabatic Chemical Reaction Triggered by Electron Photodetachment: An Ab Initio Quantum Dynamical Study. *Phys. Rev. Lett.* **2004**, *93*, 048301−4.

(17) Park, Y. C.; An, H.; Choi, H.; Lee, Y. S.; Baeck, K. K. Wave-Packet Propagation Study of the Early-Time Non-Adiabatic Dissociation Dynamics of NH_3Cl: Diabatic Picture, Effects of Isotope Substitution and Varying the Initial Vibration Levels. *Theor. Chem. Acc.* **2012**, *131*, 1212−11.

(18) Kosloff, R.; Kosloff, D. Absorbing Boundaries for Wave Propagation Problems. *J. Comput. Phys.* **1986**, *63*, 363.

(19) An, H.; Baeck, K. K. Quantum Wave Packet Propagation Study of the Photochemistry of Pheno: Isotope Effects (Ph-OD) and the Direct Excitation to the $^1\pi\sigma^*$ State. *J. Phys. Chem. A* **2011**, *115*, 13309−13315.

(20) Kling, M. F.; Vrakking, M. J. J. Attosecond Electron Dynamics. *Annu. Rev. Phys. Chem.* **2008**, *59*, 463−492.

(21) Hockett, P.; Bisgaard, C. Z.; Clarkin, O. J.; Stolow, A. Time-Resolved Imaging of Purely Valence-Electron Dynamics during a Chemical Reaction. *Nat. Phys.* **2011**, *7*, 612−615.

(22) Skone, J. H.; Soudackov, A. V.; Hammes-Schiffer, S. Calculation of Vibronic Couplings for Phenoxyl/Phenol and Benzyl/Toluene Self-Exchange Reactions: Implications for Proton-Coupled Electron Transfer Mechanisms. *J. Am. Chem. Soc.* **2006**, *128*, 16655−16663.

(23) Dutoi, A. D.; Cederbaum, L. S. An Excited Electron Avoiding a Positive Charge. *J. Phys. Chem. Lett.* **2011**, *2*, 2300−2303.

(24) Kirchner, F. O.; Gliserin, A.; Krausz, F.; Baum, P. Laser streaking of free electrons at 25 keV. *Nat. Photonics* **2014**, *8*, 52−57.